Available online at www.sciencedirect.com
ScienceDirect
Journal of the European Ceramic Society 27 (2007) 969–973
www.elsevier.com/locate/jeurceramsoc

Silicon–titanium oxycarbide glasses as bimodal porous inorganic membranes

R. Peña-Alonso[a,*], L. Téllez[b], A. Tamayo[a], F. Rubio[a], J. Rubio[a], J.L. Oteo[a]

[a] *Instituto de Cerámica y Vidrio, CSIC, c/Kelsen, No 5, Campus de Cantoblanco, 28049 Madrid, Spain*
[b] *Department Ingeniería Metalúrgica, ESIQIE-Instituto Politécnico Nacional, UPALM-Zacatenco, 07738 México, D.F. México*

Available online 5 June 2006

Abstract

Porous oxycarbide Si–Ti–O–C glasses have been studied as potential materials for inorganic membranes. Such materials were prepared by pyrolysis of hybrid materials in nitrogen atmosphere. These hybrids were synthesized by the sol–gel process using tetraethylortosilicate (TEOS), polydimethylsiloxane (PDMS) and titanium orthotitanate (TBOT) as raw material. The influence of the TEOS/TBOT molar ratio on the pore size distribution has been studied in the range of pyrolysis temperatures between 400 and 1100 °C. The oxycarbide materials were characterized by FT-IR and NMR spectroscopies, XRD, mercury porosimetry, nitrogen adsorption and SEM. Bimodal pore size distributions showed one mode close to 0.02 μm and the other one in the range between 1 and 100 μm of pore diameter. Such pore sizes increase with the amount of TBOT. Reduced effective diffusivities were calculated by a theoretical model taking into account the mentioned pore size distributions. Diffusivities appeared in the range from 0.46 to 0.77 and increase with the titanium concentration in the oxycarbide.

Keywords: Sol–gel process; Nanocomposite; Diffusion; Oxycarbide glass; Membrane

1. Introduction

During the last years a great effort has been carried out in developing silicon oxycarbide glasses.[1–4] These materials have the general formula $SiC_xO_{2-2x}+C$, where C represent the presence of free carbon. The substitution of oxygen by carbon leads to the presence of carbidic carbon units [C(Si)], which increase the bond density and, therefore, strengthen the material structure. Thus, all of the physical and chemical properties which are related to the material structure, such as glass transition temperature, chemical durability, elastic modulus and hardness, etc., are expected to increase. Silicon oxycarbide glasses are usually prepared by pyrolysis of inorganic–organic hybrid materials[1,3,5] and have potential applications as lightweight structural materials,[6] fibers, catalyst supports,[7] etc. The good thermal stability, resistance to oxidation, easy change of material composition and easy preparation make these materials attractive for many applications.

Different works have shown the preparation of porous oxycarbide glasses with a wide distribution of specific surface areas and pore volumes.[6–8] In this study, we report on the preparation of silicon–titanium oxycarbide membranes by pyrolysis in inert atmosphere of hybrid organic–inorganic preceramic materials obtained by sol–gel. The effect of the chemical composition and the pyrolysis temperature on the membrane porosities have been studied.

2. Experimental

Silicon–titanium oxycarbide membranes were obtained through the pyrolysis of thick hybrid films prepared from tetraethyl orthosilicate (TEOS) (Merck, for analysis), tetrabutyl orthotitanate (TBOT) (Aldrich, for analysis), and hydroxyl teminated polydimethylsiloxane (PDMS) (Gelest, for analysis) with average molecular weight of 550 g mol^{-1} in isopropyl alcohol and using hydrochloric acid (HCl) as catalyst. The sol–gel reaction was performed at 80 °C. Firstly a TEOS-PDMS sol was hydrolysed with HCl and H_2O and afterwards the TBOT solution was drop-wise added for half an hour in order to avoid precipitation of $Ti(OH)_4$. After 60 min spreading of the solution onto the petri dishes gave a thick film of about 200 μm that was conveniently dried up to 120 °C. Inorganic/organic mass ratio was kept constant at 70/30 and the molar ratio TEOS/TBOT was varied as follows: 70/0, 69/1, 67/3, 65/5 and 63/7, representing the samples: MST0, MST1, MST3, MST5 and MST7, respectively. The molar ratio HCl/H_2O/i-PrOH/inorganic was fixed at 0.5/3/4.5/1. The dried films were pyrolyzed at 400, 600,

* Corresponding author.
E-mail address: raquel@icv.csic.es (R. Peña-Alonso).

0955-2219/$ – see front matter © 2006 Elsevier Ltd. All rights reserved.
doi:10.1016/j.jeurceramsoc.2006.04.130

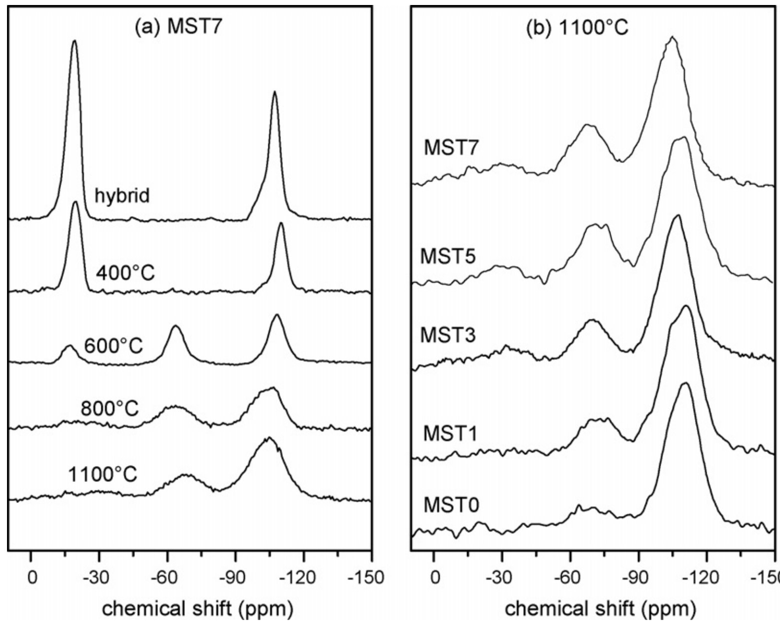

Fig. 1. ^{29}Si NMR spectra: (a) MST7 hybrid sample as-prepared and at different temperatures of pyrolysis and (b) silicon–titanium oxycarbide membranes obtained from the different titanium concentration hybrids.

800, and 1100 °C under dried nitrogen flowing at 150 ml min^{-1} forming silicon–titanium oxycarbide glass membranes.

Both hybrid films and silicon–titanium oxycarbide membranes were characterized by ^{29}Si Nuclear Magnetic Resonance (Varian NMR-400 spectrometer operating at 79.41 MHz, rotation frequency of 260 kHz, recycle delay of 15 s, 5 μs pulse and tetramethylsilane as reference), infrared spectroscopy (Perkin-Elmer FT-IR spectrophotometer 1720X with 2 cm^{-1} resolution), X-ray diffraction (XRD, Siemens D-5000 diffractometer using Cu K$_\alpha$ radiation), scanning electron microscopy (SEM, Zeiss DSM 950), mercury porosimetry (Autopore II 9215 from Micromeritics in the range of pressures between 0 and 200 MPa) and nitrogen adsorption–desorption isotherms (Tristar instrument, Micromeritics Co. at −196 °C). Elemental carbon concentration was determined by a Leco CS-200 elemental analysis instrument.

3. Results and discussion

3.1. Characterization of the hybrid films and Si–Ti oxycarbide membranes

^{29}Si NMR analysis of the as-prepared hybrid films and pyrolysed at different temperatures (Fig. 1) showed unequivocally the presence of Si–O and Si–C bonds. The signals at −20 ppm and −107 ppm in the hybrid (MST7) corresponds to D (SiO_2C_2) and Q (SiO_4) units, respectively.[9] The shoulder of the D peak is attributed to the $D(Q)$ units, i.e. polycondensation sites between PDMS molecules and Si-OH.[9,10] On the other hand, the shoulder on the Q peak has been assigned to non-polycondensed Si-OH groups from the hydrolysed TEOS.[9] Pyrolysis up to 400 °C does not vary the D signal but the Q peak (Si-OH groups) decreases due to the increase of the polycondensation degree as a result of pyrolysis. The spectrum collected at 600 °C showed the decrease of the D units and the non-presence of the Si-OH groups as a result of the redistribution reactions of PDMS molecules[5] which are also responsible of the new signal at −65 ppm assigned to the formation of T (SiO_3C) units.[5,11] The ^{29}Si NMR spectra collected at 800 and 1100 °C showed the completion of the mineralization of the network which causes the broadening of the signals associated to the different oxycarbide sites.[12]

According to Fig. 1b, which shows the ^{29}Si NMR spectra of the different oxycarbide membranes, the increase of titanium increases the signal at lower chemical shift due to the increase of SiC_4 and SiC_2O_2 oxycarbide sites whose positions are located close to −16 and −35 ppm, respectively.[12]

The FT-IR spectra (Fig. 2) confirm the observations from the ^{29}Si NMR spectra. The hybrid films showed the C–H stretching vibrations at 3000–2800 cm^{-1}, the Si–CH_3 bending at 1265 cm^{-1} and the different type of Si–O–Si stretchings at 1180, 1090 and 1030 cm^{-1} $D(Q)$ units of ^{29}Si NMR corresponds to the peak centred at 850 cm^{-1}. The bending vibrations of SiX_4^- (X = C, O) and O–Si–O bonds appears at 800 and 410 cm^{-1}, respectively.

Redistribution and mineralization reactions transform the hybrid films into inorganic materials produce the changes of the FT-IR spectra:[5] C–H bonds disappear as CH_4 and H_2 are formed and removed by the flow carrier gas, the Si–CH_3 groups of PDMS evolve to Si–C–Si bonds which form the silicon oxycarbide structure.[1,3,4] The presence of higher amounts of TBOT develops a weak shoulder between 900–850 cm^{-1} attributed to the Si–C stretching vibration[13] indicating the increase of carbidic carbon units [C(Si)].

The carbon content continuously decrease with the pyrolysis temperature independently on the TBOT concentration. The 20 wt.% C of the films decreases up to 1.90, 191, 1.98, 2.05 and 2.17 wt.% C respectively for the MST0, 1, 3, 5 and 7 oxycarbide

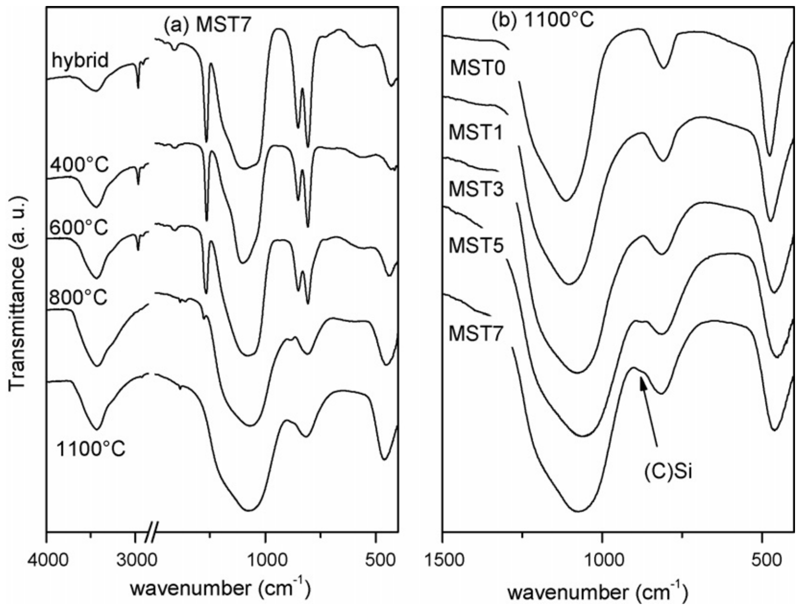

Fig. 2. FT-IR spectra: (a) MST7 hybrid sample as-prepared and at different temperatures of pyrolysis and (b) silicon–titanium oxycarbide membranes with different titanium content.

membranes obtained at 1100 °C. This is due to the redistribution and mineralization reactions occurring during the hybrid-to-oxycarbide material transformation. The low carbon content of the membranes arises from the difficulty to retain carbon in both thick and thin films, as it was showed by Colombo et al.[14] but, according to the SiC_xO_y signals of the NMR spectra, most of this carbon can be found in the oxycarbide network.

SEM micrographs showed that the processed silicon oxycarbide glass membranes are homogeneous and display a thickness of about 160 μm (Fig. 3a). The as-prepared hybrid films exhibit shrinkage of about 20% during pyrolysis and the microstructure of the final membranes appears to be formed of small spherical particles of about 200 nm (Fig. 3b).

The hybrid preceramic films showed low specific surface area (SSA) values, ranging from 26 $m^2\,g^{-1}$ for the MST0, to 89 $m^2\,g^{-1}$ for the MST7 sample (Table 1). These values increase up to 470 $m^2\,g^{-1}$ when the pyrolysis is carried out at 400 °C, showing the formation of micropores during treatment but higher temperatures causes the decrease of the SSAs. On the other hand, SSAs of silicon–titanium oxycarbide membranes (Table 1) show values very close to that obtained for unsupported SiO_2-based hybrid membranes.[15] Therefore, low amounts of TBOT (1%) causes an increase of the SSA whereas additions of higher amounts of this alkoxide make continuously decrease the SSA values, a result that can be associated to the catalytic effect of the TBOT on polymers such as PDMS.[16]

Mesopore size distributions have been obtained by using the Barret–Joyner–Halenda (BJH) method applied to the nitrogen adsorption isotherms[17] while macropore size distributions (pores with sizes between 50 nm and 100 μm) have been obtained from mercury intrusion measurements.[18] PSD presents two modes: one in the range of mesopores and the other in the macropore region which are given in Table 1. Addition of TBOT produces opposite effects in such mean pore sizes. Thus, for the MST0 oxycarbide membrane the mesopore mode is located at about 2.9 nm and the macropore one at 50 μm. Taken into account that the membrane thickness is close to 160 μm, the presence of the macropore mode must be associated to the formation of bubbles interconnected with mesopores. The mesopore mode is very close to that obtained for other hybrid and inorganic

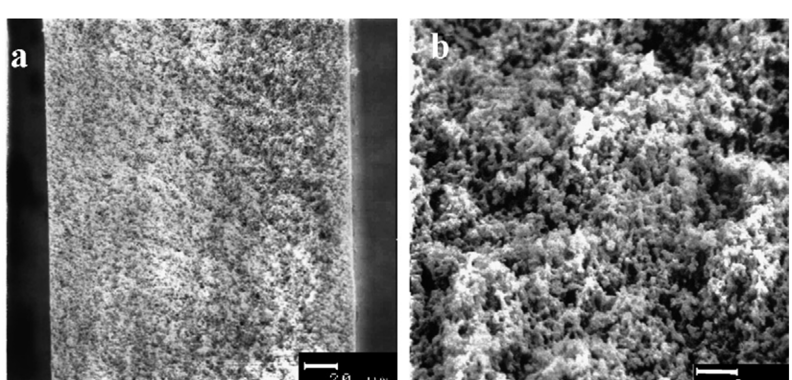

Fig. 3. SEM micrograph of a silicon–titanium oxycarbide membrane.

Table 1
SSA, pore volume and effective diffusion coefficient (D_{re}) values for silicon–titanium oxycarbide membranes

Sample	SSA ($m^2 g^{-1}$)	Pore volume ($cm^3 g^{-1}$)	Mean pore size		D_{re}
			Mesoporous (nm)	Macroporous (μm)	
MST0	77.36	0.28 + 0.08 = 0.36	2.9	50.7	0.46
MST1	94.58	0.18 + 0.15 = 0.33	5.9	19.2	0.54
MST3	61.15	0.12 + 0.27 = 0.39	6.9	16.6	0.53
MST5	59.06	0.17 + 0.36 = 0.53	15.5	6.5	0.61
MST7	54.81	0.29 + 0.49 = 0.78	45.8	1.7	0.77

membranes.[15,19] The increase of TBOT results in the increase of the mesopore diameter and the decrease of the macropore one while the inverse trend is observed for the intensities of both modes. Then, the mesopore mode increases from 2.9 to 45.8 nm and the macropore mode decreases from 50 to 1.7 μm, from the MST0 to the MST7 silicon–titanium oxycarbide membranes. Thus, silicon–titanium oxycarbide membranes of very different pore size modes can be prepared by adding concentrations of TBOT up to 7 wt.% (Fig. 4).

3.2. *Effective diffusivity of silicon–titanium oxycarbide membranes*

Effective application of porous solids in sorption depends markedly on their interparticle mass transport abilities, quantified by the effective diffusion coefficient. If the porosity of the prepared silicon–titanium oxycarbide membranes is taken into account, moderate mass transport properties may be expected.[20] Using the effective medium theory, Burganos and Sotirchos[21] developed a convenient and reliable method for calculation of the effective diffusivity in porous solids. Neglecting Knudsen diffusion coefficient, the effective diffusivity in a porous structure is given by:

$$D_{ef} = \frac{D[\varepsilon(d^2)_e]}{\tau(d^2)} \tag{1}$$

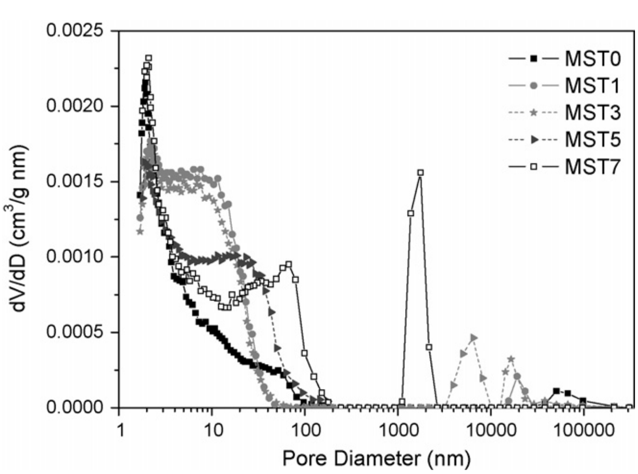

Fig. 4. Pore size distributions (PSD) obtained from nitrogen gas desorption isotherms and mercury porosimetry results for the silicon–titanium oxycarbide membranes prepared by pyrolysis at 1100 °C of the corresponding hybrid films.

where ε is the porosity, D the bulk diffusion coefficient, τ the tortuosity factor, and $(d^2)_e$ and (d^2) are calculated from the equations:

$$\int_d \frac{d^2 - (d^2)_e}{d^2 - (Z/2 - 1)(d^2)_e} n(d)\,\mathrm{d}d = 0 \tag{2}$$

$$(d^2) = \frac{\int_d d^2 n(d)\,\mathrm{d}d}{\int_d n(d)\,\mathrm{d}d} \tag{3}$$

where $n(d)$ is the pore number distribution computed for a cylindrical pore geometry and Z the mean coordination number or pore connectivity. The effect of the pore network structure on the effective diffusivity may be better estimated using normalized values, i.e. the reduced effective diffusivities, D_{re}:

$$D_{re} = \frac{D_{ef}}{D\varepsilon/\tau} = \frac{(d^2)_e}{(d^2)} \tag{4}$$

Diffusivities correspond to the above mentioned mesopore mode of the PSDs. D_{re} estimated for the MST0 hybrid film exhibits a value of 0.71 which changes to 0.83, 0.63, 0.48 and 0.46 at the pyrolysis temperatures of 400, 600, 800 and 1100 °C, respectively. This behaviour agrees with the porosity formed or removed during the pyrolysis process. D_{re} of the oxycarbide membranes (see Table 1) are close to those estimated for conventional silica or alumina porous supports[22] and are lower than those estimated for silica aerogels.[20] Therefore, these data clearly confirm the possibility of producing silicon–titanium oxycarbide glasses to be used as membranes for liquid and gases.

4. Conclusions

Silicon–titanium oxycarbide membranes have been obtained by pyrolysis of hybrid organic–inorganic materials. The increase of titanium produces an increase of the SiO_2C_2 and SiC_4 units. The membranes presented bimodal porosity in which the mesopore volume decreases whereas diameter increases with the increase of titanium content.

The calculated effective diffusivities increase with the pore diameter, i.e., with the amount of titanium forming the membrane. Thus, low variations of titanium concentrations on the silicion oxycarbide membranes caused very different pore size distributions and, therefore, different diffusivities of such membranes.

Acknowledgments

This research has been possible by financial support from Comisión Interministerial de Ciencia y Tecnología of Spain (CICYT, Project Ref. MAT2002-03891) and. L. Téllez is grateful to the Instituto Politécnico Nacional and the Consejo Nacional de Ciencia y Tecnología (CONACyT) of Mexico for the grant ref. 72432).

References

1. Pantano, C. G., Singh, A. K. and Zhang, H., Silicon oxycarbide glasses. *J. Sol–gel Sci. Technol.*, 1999, **14**, 7–25.
2. Renlund, G. M. and Prochazka, S., Silicon oxycarbide glasses. Part II. structure and properties. *J. Mater. Res.*, 1991, **6**, 2723–2734.
3. Soraru, G. D., Silicon oxycarbide glasses from gels. *J. Sol–gel Sci. Technol.*, 1994, **2**, 843–848.
4. Turquat, C., Bréquel, H., Kleebe, H. J., Babonneau, F. and Enzo, S., Investigation of SiCO glasses synthesized with extensive ball milling. *J. Non-cryst. Solids*, 2003, **319**, 117–128.
5. Belot, V., Corriu, R. J. P., Leclercq, D., Mutin, P. H. and Vioux, A., Thermal reactions occurring during pyrolysis of crosslinked polysiloxane gels, precursors to silicon oxycarbide glasses. *J. Non-cryst. Solids*, 1992, **147/148**, 52–55.
6. Schmidt, H., Kock, D., Grathwohl, G. and Colombo, P., Micro-macroporous ceramic from preceramic precursors. *J. Am. Ceram. Soc.*, 2001, **84**, 2252–2255.
7. Singh, A. K. and Pantano, C. G., Porous silicon oxycarbide glasses. *J. Am. Ceram. Soc.*, 1996, **79**, 2696–2704.
8. Liu, C., Zhang, H., Komarneni, S. and Pantano, C. G., Porous silicon oxycarbide glasses from organically modified silica gels of high surface area. *J. Sol–gel Sci. Technol.*, 1994, **1**, 141–151.
9. Iwamoto, T., Morita, K. and Mackenzie, J. D., Liquid state ^{29}Si NMR study on the sol–gel reaction mechanisms of ormosils. *J. Non-cryst. Solids*, 1993, **159**, 65–72.
10. Babonneau, F., NMR characterization of hybrid siloxane-oxide materials. *New J. Chem.*, 1994, **18**, 1065–1071.
11. Zhang, H. and Pantano, C. G., Synthesis and characterization of silicon oxycarbide glasses. *J. Am. Ceram. Soc.*, 1990, **73**, 958–963.
12. Sorarù, G. D., D'Andrea, G., Campostrini, R., Babonneau, F. and Mariotto, G., Structural characterization and high-temperature behavior of silicon oxycarbide glasses prepared form sol–gel precursors containing Si–H bonds. *J. Am. Ceram. Soc.*, 1995, **78**, 379–387.
13. Hasegawa, I., Nakamura, T., Motojima, S. and Kajiwara, M., Síntesis of silicon carbide fibers by sol–gel processing. *J. Sol–gel Sci. Technol.*, 1997, **8**, 577–579.
14. Colombo, P., Paulson, T. E. and Pantano, C. G., Atmosphere effects in he processing of silicon carbide and silicon oxycarbide thin films and coatings. *J. Sol–gel Sci. Technol.*, 1994, **2**, 601–604.
15. Dirè, S., Pagani, E., Babonneau, F., Ceccato, R. and Carturan, G., Unsupported SiO_2-based organic-inorganic membranes. Part 2. Surface features and gas permeation. *J. Mater. Chem.*, 1997, **7**, 919–922.
16. Andrianov, K. A., Polymers with inorganic primary molecular chains. *J. Polym. Sci.*, 1961, **52**, 257–276.
17. Barrett, E. P., Joyner, L. G. and Halenda, P. P., The determination of pore volume and area distributions in porous substances. I. Computations from nitrogen isotherms. *J. Am. Chem. Soc.*, 1951, **73**, 373–380.
18. Pirard, R., Sahouli, B., Blacher, S. and Pirard, J. P., Sequentially compressive and intrusive mechanisms in mercury porosimetry of carbon blacks. *J. Colloid Interf. Sci.*, 1999, **217**, 216–217.
19. Sekulic, J., Luiten, M. W. J., ten Elshof, J. E., Benes, N. E. and Keizer, K., Microporous silica and doped silica membrane for alcohol dehydration by perevaporation. *Desalination*, 2002, **148**, 19–23.
20. Jarzebski, A. B. and Lorenc, J., Pore network connectivity and effective diffusivity of silica aerogels. *Chem. Eng. Sci.*, 1995, **50**, 357–360.
21. Burganos, V. N. and Sotirchos, S. V., Diffusion in pore networks: effective medium theory and smooth field approximation. *AIChE J.*, 1987, **33**, 1678–1689.
22. Liu, H., Zhang, L. and Seaton, N. A., Determination of the connectivity of porous solids from nitrogen sorption measurements. II. Generalisation. *Chem. Eng. Sci.*, 1992, **47**, 4393–4404.